A Planar-Lumped Model for Coupled Microstrip Lines and Discontinuities

Albert Sabban and K. C. Gupta, *Fellow, IEEE*

Abstract—**This paper presents a convenient model for analyzing coupled microstrip line discontinuities. Similar to the planar waveguide model for single microstrip lines, a planar-lumped model is developed for coupled microstrip lines. Fields underneath the two strips and those fringing at the outer edge are modeled by two equivalent planar waveguides. Electric and magnetic field coupling in the gap region is modeled by a lumped network. The lumped network parameters are evaluated such that [*C*] and [*L*] matrices for the model are identical with those for coupled lines. The model is verified by comparing coupler characteristics with those obtained by the conventional coupled line analysis. Just as the planar model of a single microstrip has been used for characterizing microstrip discontinuities, the planar-lumped model developed here is used for coupled line discontinuities. Examples given here include a coupled microstrip section with chamfered right-angled bends to single microstrip lines, for which the results are in good agreement with experimental values.**

I. Introduction

SECTIONS of coupled microstrip lines are used extensively for design of directional couplers, filters and other components in hybrid and monolithic microwave circuits [1], [2]. Although characteristics of uniform coupled lines have been studied extensively [3], characterization of discontinuities and junctions in coupled lines is not readily available. Open-end is perhaps the only coupled microstrip line discontinuity described in detail [4]. Specifically, there is a need for characterization of junctions from coupled line sections to outgoing single microstrip lines connected to other components in the circuit.

The purpose of this paper is to present a model suitable for characterization of several of the coupled-line junction configurations. The role of this model is similar to that of the planar waveguide model for single microstrip lines, a model that has been used extensively for characterization of several microstrip discontinuities like bends, chamfered bends, tee-junctions and cross-junctions etc. [5], [6]. The proposed model is a combination of two-dimensional planar and lumped-element networks. Fields underneath the two strips and those fringing at the outer-edges are modeled by planar waveguides. The electric field and magnetic field couplings across the gap are represented by an equivalent capacitive and inductive lumped network. Various model parameters are determined such that [*C*] and [*L*] matrices for the model are identical to those for the coupled microstrip section.

Manuscript received February 28, 1991; revised August 2, 1991. This work was supported by the Center for Microwave/MM-Wave CAD at the University of Colorado at Boulder.

The authors are with the Department of Electrical and Computer Engineering, the University of Colorado at Boulder, Boulder, CO 80309-0425.

IEEE Log Number 9105251.

II. The Planar-Lumped Model for Coupled Microstrip Lines

A coupled microstrip section and the proposed planar-lumped model is shown schematically in Fig. 1. Fields underneath the two strips and fringing fields at the outer edges e_1 are represented by two planar waveguides (with magnetic walls) characterized by multiport *Z*-matrices Z_A and Z_B respectively. Fields in the gap between the two lines (including the fringing fields associated with the inner edges e_2) are modeled by the lumped network shown in the figure. Selection of various parameters ensures that the capacitance and inductance matrices for the coupled line configuration and its model are identical.

A. Planar Waveguides Parameters

For the coupled microstrip line model, the planar waveguides (shown in Fig. 1) account for fringing fields only at the outer edges. So their effective widths $W_e(f)$ are chosen to account for outward extension at outer edges only. We get

$$W_e(f) = \frac{W_{em}(f) + W}{2} \tag{1}$$

where W is the physical width for the two lines. The dielectric constant for planar waveguide segments is taken to be equal to ϵ_{re} for isolated microstrip lines of width W. W_{em} is the effective width of the equivalent planar waveguide for a single microstrip line, given by [5]

$$W_{em}(f) = \eta_0 h / \{Z_0(f)\sqrt{\epsilon_{re}(f)}\} \tag{2}$$

where η_0 is the intrinsic wave impedance ($120\pi\ \Omega$) of free space and h is the height of the substrate. $Z_0(f)$ and $\epsilon_{re}(f)$ are the frequency dependent characteristic impedance and effective dielectric constant values obtained from microstrip line analysis. The two planar waveguide segments in Fig. 1 are connected together through a multiport lumped network as shown in Fig. 1. Lengths of these planar seg-

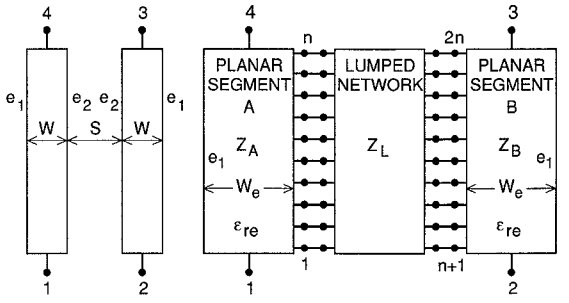

Fig. 1. A coupled line section and its planar-lumped model.

ments are equal to the physical length of the coupled line section. If there are n ports on each of the inner edges, each planar waveguide segment is characterized by a $(n + 2$ by $n + 2)$ impedance matrix (assuming that we are considering only one port at each end of the coupled line section). Z-matrices for the two planar waveguide sections are derived from two-dimensional Green's function for rectangular geometry and account for all the higher (z-invariant) two-dimensional modes present in these regions.

B. C-Network for Modeling E-Field Coupling

The lumped network representing the electric field coupling between the two strips is derived from the capacitance matrix for the coupled microstrip lines. The capacitance matrix for coupled microstrip lines is obtained from electromagnetic analysis of coupled microstrips. An analysis algorithm based on Bryant and Weiss method [7] was used for computations reported in this paper. However, in order to include the dispersion effects in the planar-lumped model for coupled line, the spectral domain approach [3] may be used to calculate the frequency dependent even and odd mode characteristic impedances and effective dielectric constants. Even and odd mode capacitances (C_e and C_0) are related to the even and odd mode characteristic impedances (Z_{0e} and Z_{00}) and corresponding velocities [1].

For a purely capacitive multiport network, the C-matrix may be defined as $\boldsymbol{i} = j\omega[C]\,\boldsymbol{V}$ where $\boldsymbol{i}$ and $\boldsymbol{V}$ are vectors representing port currents and port voltages respectively. Even and odd mode capacitances (C_e and C_0 respectively) are related to the $[C]$ matrix as follows:

$$[C] = \begin{bmatrix} C_{11} & C_{12} \\ C_{21} & C_{22} \end{bmatrix} = \begin{bmatrix} \dfrac{C_e + C_0}{2} & \dfrac{C_e - C_0}{2} \\ \dfrac{C_e - C_0}{2} & \dfrac{C_e + C_0}{2} \end{bmatrix} \quad (3)$$

A π-network representation of the $[C]$ matrix for a coupled line section of length Δl is shown in Fig. 2(a). For the model proposed (Fig. 1), the shunt capacitance $C_{sh} = C_{11} + C_{12}$ is accounted for partially by the planar segment (with $[Z] = [Z_a]$). The remaining part of C_{sh} is modeled by the element C_f of the lumped network representing the coupling gap. A section of this network is shown in Fig. 2(b). C_f is found to be

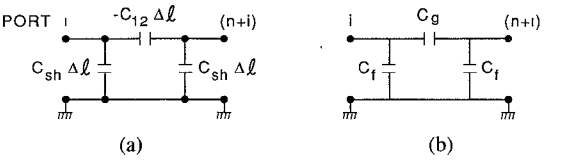

Fig. 2. C-network representation for modeling E-field coupling. (a) π-matrix representation of $[C]$ for coupled lines section of length Δl. (b) A section of the capacitive part of the lumped network.

$$C_f = \left(C_{sh} - \frac{\epsilon_0 \epsilon_{re} W_e}{h}\right) \Delta l = \left(C_e - \frac{\epsilon_0 \epsilon_{re} W_e}{h}\right) \Delta l \quad (4)$$

where Δl is the length of the line represented by the port i. The matrix $[C]$ represents capacitances per unit length of the line. The network section shown in Fig. 2(b) may be represented by the following Y-matrix:

$$[Y_C] = j\omega \begin{bmatrix} C_f + C_g & -C_g \\ -C_g & C_f + C_g \end{bmatrix} = j\omega[C_G] \quad (5)$$

where $C_g = -C_{12}\,\Delta l$. When the lumped network of Fig. 1 has n ports on each side, the complete C-matrix C_G may be written as shown in Table I. Non-diagonal terms in each of the four sub-matrices are all zeros.

C. L-Network for Modeling H-Field Coupling

The magnetic field coupling between the two strips is modeled by mutual inductance elements in the lumped network. If we consider two adjacent ports of planar waveguide network A (say 1 and 2) facing the two corresponding ports $(n + 1)$ and $(n + 2)$ of the planar subnetwork B, the inductive coupling network for this portion may be drawn as shown in Fig. 3(a). Values of L_p and M are calculated by comparing the $[L]$-matrix of the coupling line with that for the modeling network. The inductance matrix for the coupled line is obtained from the capacitance matrix $[C_0]$ for the case when the dielectric is replaced by air. We have the following relation between $[L]$ and $[C_0]$ matrices:

$$[L] = \begin{bmatrix} L_{11} & L_{12} \\ L_{21} & L_{22} \end{bmatrix} = \mu_0 \epsilon_0 [C_0]^{-1} \left[\frac{\text{Henry}}{m}\right] \quad (6)$$

where μ_0 and ϵ_0 are permeability and permittivity of the free space. The network representation of the inductance matrix in (6) is shown in Fig. 3(b). Here Δl is the length of the section represented by the partial network shown and $[L]$ is the matrix of inductances per unit length of the coupled line. A part of the $\Delta l L_{11}$ is contributed by the inductance of the planar waveguide and the remaining by L_p included in the lumped network as shown in Fig. 3(a) and (c). If the inductance of the planar waveguide region per unit length $(= \mu_0 h / W_e)$ is denoted by L_{pl}, the total inductance network may be drawn as shown in Fig. 3(c). Equating the admittance matrices of the two networks shown in Fig. 3(b) and (c), L_p and M are expressed in

TABLE I
C-MATRIX FOR THE LUMPED NETWORK MODELING THE GAP

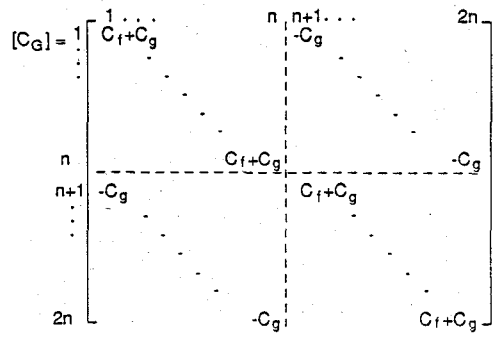

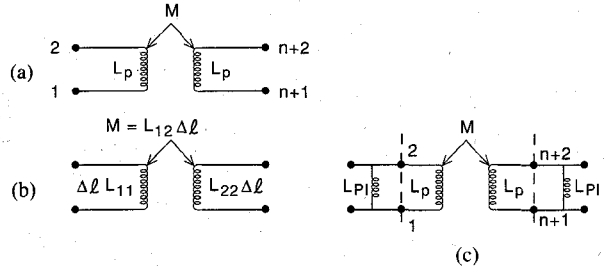

Fig. 3. *L*-network representation for modeling *H*-field coupling. (a) A section of the inductive network in the lumped network for the gap. (b) Network representation for inductance matrix of a section Δl of the coupled line. (c) Network (for the coupled lines) with self inductance contributions of planar segment and lumped network shown separately.

terms of Lpl and $[L]$ as follows:

$$L_p = \frac{L_{11} - (L_{11}^2 - L_{12}^2)/L_{pl}}{1 - 2L_{11}/L_{pl} + (L_{11}^2 - L_{12}^2)/L_{pl}^2} \Delta l \text{[Henry]} \quad (7)$$

and

$$M = \frac{L_{12}\,\Delta l}{1 - 2L_{11}/L_{pl} + (L_{11}^2 - L_{12}^2)/L_{pl}^2} \text{[Henry]}. \quad (8)$$

In these expressions we have used $L_{12} = L_{21}$ and it is assumed that $L_{11} = L_{22}$ (symmetric lines). Formulation could, of course, be extended to asymmetric lines also by having $L_{11} \neq L_{22}$. The complete inductive part of the lumped network portion of the model is shown in Fig. 4. In this network, half inductance sections at the terminal ports (1, 2, $n + 1$, $2n$) are also included. Therefore, the lumped network representing the gap is a $(2n + 4)$ port network. The $2n + 4$ port admittance matrix of this network is obtained by using Kirchhoff's laws and may be written as follows:

$$[Y_L] = \frac{-j}{\omega(L_p^2 - M^2)} [L_G] \quad (9)$$

where $[L_G]$ is the corresponding inductance matrix shown in Table II. It may be noted that all the four $(n \times n)$ submatrices are tridiagonal, with all other off-diagonal elements being zero.

The total lumped network required for modeling the gap is obtained by superposition of capacitive and inductive components. The total admittance matrix of this network is obtained by adding $[Y_C]$ and $[Y_L]$ given by (5) and (7) respectively. We have the admittance matrix of the gap network $[Y_G]$ given by

$$[Y_G] = [Y_C] + [Y_L] = j\omega[C_G] - \frac{j}{\omega(L_p^2 - M^2)} [L_G]. \quad (10)$$

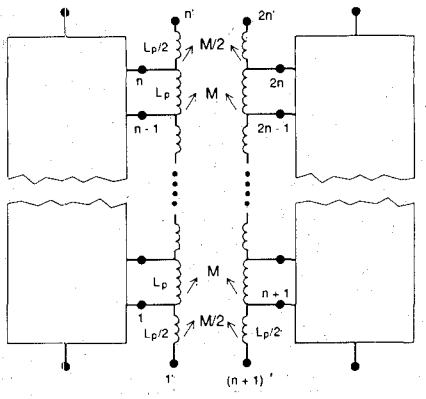

Fig. 4. *L*-network representing inductive coupling across the gap.

III. Model Verification for the Dominant Mode

The planar-lumped model for coupled microstrip lines proposed in Section II has been verified by considering a quarter-wave section of coupled microstrips, finding its 4-port parameters based on the proposed model, and comparing these with the four-port parameters obtained by conventional coupled line analysis [9]. The starting point for both of these computations is the values of the even and odd mode impedances and effective dielectric constants which are obtained from the Bryant and Weiss algorithm [7].

In conventional coupled-line computations, non-equality of even and odd mode phase velocities has been taken into account for obtaining 4-port *S*-parameters. The configuration considered is a coupled microstrip lines section (with each of 50 Ω characteristic impedance in isolation) on 0.254 mm thick substrate with $\epsilon_r = 2.2$. The length of this section is equal to $\lambda/4$ (for isolated lines) at 10 GHz. Spacing between the parallel lines was varied from 0.1 to 20 times the substrate thickness and the coupling parameter S_{21} calculated for various cases.

Comparison for the case of coupling coefficient S_{21} values obtained from the proposed model and those from conventional analysis is shown in Fig. 5. The two curves coincide and cannot be distinguished in the figure. This very good agreement and similar agreements for other *S*-parameters provide a verification for the proposed model for the dominant even and odd modes.

IV. Model Verification for Higher-Order Modes

It has been shown [5] that the planar waveguide model for single microstrip lines predicts the higher-order modes of microstrip lines fairly accurately. In this section it is

TABLE II
L-MATRIX FOR THE LUMPED NETWORK MODELING THE GAP

	1	2	3	4	...	n-1	n	n+1	n+2	n+3	n+4	n+5	...	2n	2n+1	2n+2	2n+3	2n+4
1	$2L_p$	$-2L_p$	0							$-2M$	$2M$							
2	$-2L_p$	$3L_p$	$-L_p$							$2M$	$3M$	M						
3	0	$-L_p$	$2L_p$	$-L_p$							M	$-2M$	M					
4			$-L_p$	$2L_p$														
n-1																		
n							$-L_p$	$2L_p$	$-L_p$							$-2M$	M	
n+1								$-L_p$	$3L_p$ $-2L_p$							M	$3M$	$2M$
n+2								0	$-2L_p$ $2L_p$							0	$2M$	$-2M$
n+3	$-2M$	$2M$								$2L_p$	$-2L_p$							
n+4	$2M$	$3M$	M							$2L_p$	$3L_p$	$-L_p$						
n+5		M	$-2M$	M						0	$-L_p$	$2L_p$ $-L_p$						
2n												$-L_p$	$2L_p$					
2n+1																		
2n+2							$-2M$	M							$-L_p$	$2L_p$	$-L_p$	
2n+3							M	$3M$	$2M$							$-L_p$	$3L_p$	$-2L_p$
2n+4							0	$2M$	$-2M$							0	$-2L_p$	$2L_p$

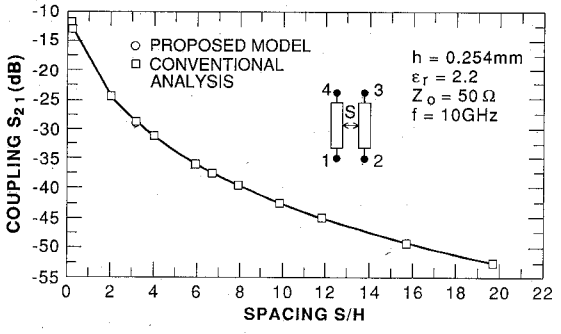

Fig. 5. Comparison of coupling computed by planar-lumped model with conventional coupled line analysis.

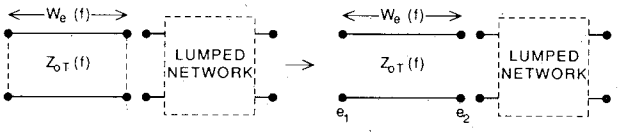

Fig. 6. Planar waveguide model of one of the coupled microstrip lines with the lumped network for gap coupling and its equivalent transmission line model in the transverse direction.

shown that the planar-lumped model for coupled microstrips is valid for the higher-order modes for coupled microstrip lines also. Cut-off frequencies for higher-order modes are evaluated by transverse resonance method applied to the proposed model and compared with the corresponding values obtained from the spectral domain analysis for higher order modes of coupled microstrips.

The planar waveguide model consists of two parallel waveguides terminated by magnetic walls (at the outer edges e_1) in the transverse directions. In terms of network theory, a magnetic wall is an open circuit. In the transverse direction, the planar waveguide section of extent Δl may be represented as an open-circuited transmission line with length $W_e(f)$ and effective dielectric constant ϵ_{re} as shown in Fig. 6. Here $W_e(f)$ is given by (1). The characteristic impedance Z_{0T} corresponds to a planar waveguide of width Δl and is given by

$$Z_{0T}(f) = 1/Y_{0T}(f) = \frac{\eta_0 h}{\Delta l \sqrt{\epsilon_{re}(f)}}. \tag{11}$$

The open circuit (zero admittance) at the outer edge e_1 (Fig. 1) is transformed to an admittance seen at the location of the inner edge e_2. $Y_i(e_2)$ is given by

$$Y_i(e_2) = jY_{0T}(f) \tan \beta W_e(f) \tag{12}$$

where $\beta = k_0\sqrt{\epsilon_{re}}$, k_0 is the wave number in free space and ϵ_{re} is the effective dielectric constant for planar waveguides in the model as discussed earlier. The transverse resonance network for the planar-lumped model is shown in Fig. 7(a) and is used for evaluating cut-off frequencies for higher-order modes in coupled microstrip lines.

For study of even and odd modes, the mutual inductance elements in Fig. 7(a) are represented by equivalent *Y*-networks as shown in Fig. 7(b). It can be shown that the *Y*-network in Fig. 7(b) is equivalent to coupled in-

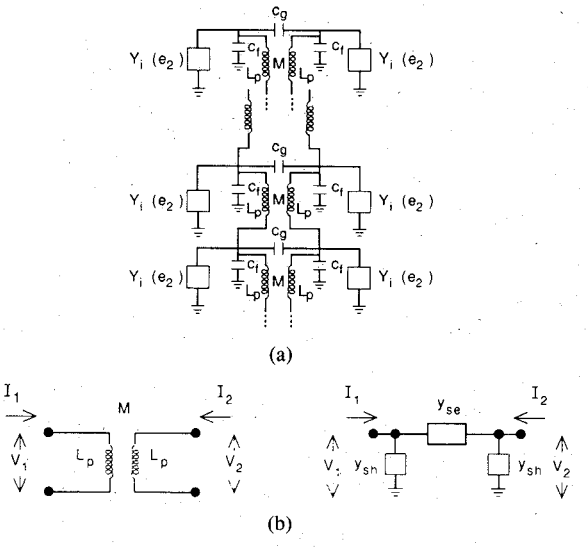

Fig. 7. (a) Network model to evaluate transverse resonance frequencies. (b) Y-network representation of mutual inductance element.

ductances when

$$Y_{sh} = \frac{1}{j\omega(L_p + M)} \tag{13}$$

and

$$Y_{se} = \frac{M}{j\omega(L_p^2 - M^2)}. \tag{14}$$

The transverse network used to evaluate cut-off frequencies for higher-order modes in coupled lines may be represented as shown in Fig. 8.

Using even and odd mode analysis, the network representation in the transverse direction for the even and odd modes is shown in Fig. 9. Part of the fringing fields network representing elements common to even and odd modes may be represented by an additional parallel plate line in the Z-direction with Z_{0f} given by

$$Z_{0f} = \sqrt{\frac{L_p + M}{C_f}} = 1/Y_{0f}. \tag{15}$$

Using (11), equivalent width W_{ef} and effective dielectric constant ϵ_{rf} for this line may be written as

$$W_{ef} = \frac{\eta_0 h}{Z_{0f}\sqrt{\epsilon_{rf}}} \tag{16}$$

$$\epsilon_{rf} = \frac{(L_p + M)C_f}{\mu_0 \epsilon_0 \Delta l^2}. \tag{17}$$

The transverse resonance for the even and odd modes takes place when the susceptance to the left of plane e_2 is equal to the negative of the susceptance to the right of plane e_2. For even mode this is given by the following transcendental equation:

$$Y_{0T} \tan\left(\frac{2\pi}{c} f \sqrt{\epsilon_{re}(f)}\, W_e(f)\right) + Y_{0f} \tan\left(\frac{2\pi}{c} f \sqrt{\epsilon_{rf}} W_{ef}\right) = 0. \tag{18}$$

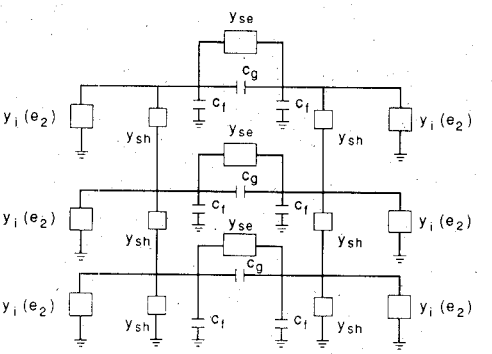

Fig. 8. Transverse resonance network used to evaluate cut-off frequencies of higher order modes.

For odd mode, the standard transmission line formula is used to find the admittance to the right of point e_2 where the terminating impedance Z_L (at the end of a line of length W_{ef} and $Z_0 = Z_{0f}$) is given by

$$Z_L = \left(\frac{2M}{j\omega(L_p^2 - M^2)} + 2j\omega C_g\right)^{-1}. \tag{19}$$

The higher-order mode cut-off frequencies are obtained by using a root searching routine to solve for f from the transcendental equation (18) for even modes and a similar equation for the odd modes.

In order to verify that the proposed model predicts higher-order modes in coupled lines, we compared results for the cutoff frequency of higher-order modes obtained using the planar-lumped model approach with results obtained using the spectral domain approach for the analysis for higher-order modes of the coupled lines. Results for cutoff frequencies for higher-order modes of coupled lines on 0.635 mm thick substrate with $\epsilon_r = 9.7$, (line width of 9.15 mm and the spacing between the strips is 0.635 mm) are listed in Table III. Based on this fairly good agreement between spectral domain results and the planar-lumped model results, we conclude that the model developed is valid not only for the dominant even and odd modes but also for higher-order even and odd modes. This forms the basis for using the proposed model for characterization of coupled microstrip discontinuities which cause excitation of higher-order modes also.

V. Comparison with Experimental Results for a Coupled Line Section with Chamfered Bends

The coupled microstrip line model proposed above has been applied for characterization of the junctions between coupled line sections and single microstrips located at right angles to the ends of the coupled line section as shown in Fig. 10(a). The planar-lumped model for this configuration is shown in Fig. 10(b). In addition to the three segments (two rectangular plus a lumped network) representing the coupled line section, we have three additional planar segments at each of the two upper ports (1 and 2).

The network model shown in Fig. 10(b) is analyzed by the commonly used segmentation method [18] and the re-

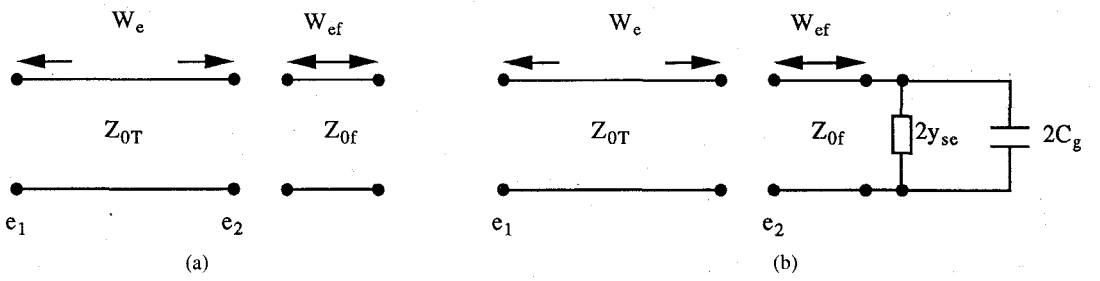

Fig. 9. Equivalent transmission line representations in the transverse direction for (a) even modes and (b) odd modes.

TABLE III
CUT-OFF FREQUENCIES IN (GHz) FOR HIGHER-ORDER MODES IN COUPLED LINES (DIMENSIONS GIVEN IN THE TEXT)

		Cut-Off Frequencies		
Planar Lumped Model	Even Mode	5.290	10.588	15.950
	Odd Mode	5.230	10.790	15.937
Spectral Domain Analysis	Even Mode	5.300	10.700	15.940
	Odd Mode	5.100	10.760	15.900

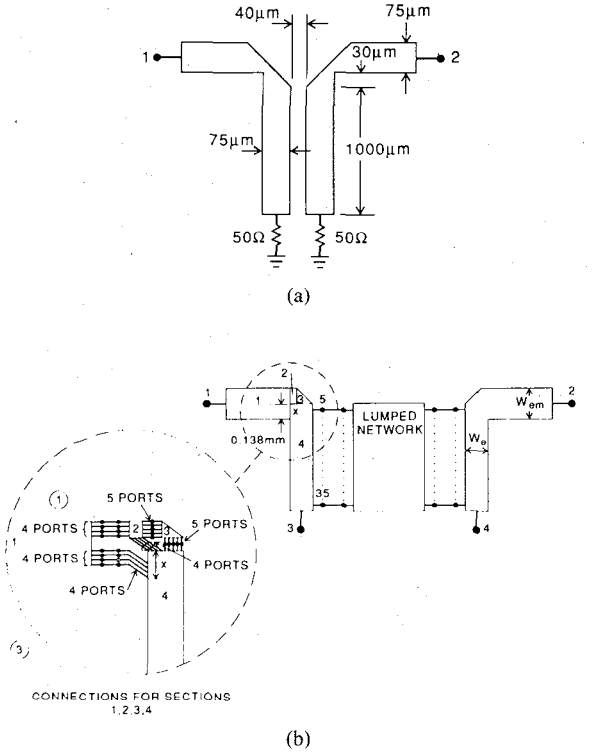

Fig. 10. (a) A coupled microstrip section with chamfered bends. (b) Planar-lumped model for coupled line configuration of Fig. 10(a).

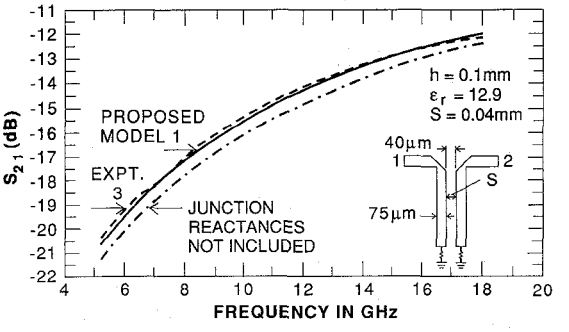

Fig. 11. Comparison of S_{21} values for coupled line configuration of Fig. 10 as obtained by: 1) planar-lumped model, 2) conventional coupled line analysis, and 3) measurements.

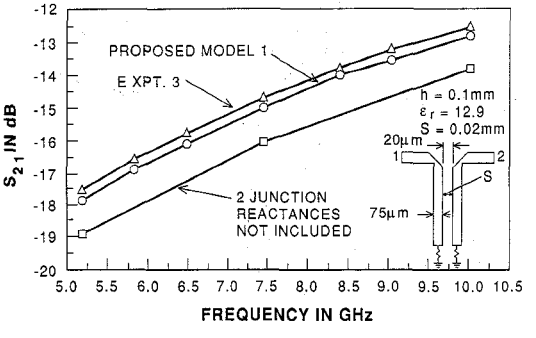

Fig. 12. Comparison of S_{21} values for coupled line configuration of Fig. 10 as obtained by: 1) planar-lumped model, 2) conventional analysis, and 3) measurements, all for spacing of 20 μm.

sults obtained are compared with the experimental results for the structure fabricated on 4 mil thick GaAs substrate (ϵ_r = 12.9). Comparison for the transmission coefficient S_{21} is shown in Fig. 11(a). The curve marked 1 shows computed results, curve 3 shows experimental results, and curve 2 shows the results without taking junction reactance into account. The data for curve 2 is obtained from transmission line analysis of coupled lines.

Results of S_{21} for the structure shown in Fig. 10 with spacing of 20 μm between the strips are plotted in Fig. 12. In this figure the curve marked 1 shows computed S_{21} results, curve 3 shows measured S_{21} results and curve 2 shows computed S_{21} results without taking junction reactances into account. The differences between measured S_{21} results and computed S_{21} results, using the planar-lumped model, at 5.2 GHz and 10 GHz are 0.36 dB and 0.32 dB respectively. The differences between measured S_{21} results and computed S_{21} results, using transmission line analysis, at 5.2 GHz and 10 GHz are 1.05 dB and 1.27 dB respectively.

Good agreement between computed and experimental results verifies the modeling procedure developed and its

applications to the characterization of coupling line discontinuities.

VI. Comparison with Fullwave Analysis for a Coupler with Four Chamfered Bends

In this section, the planar-lumped model results are compared to fullwave analysis results obtained from P-Mesh code [12]. The planar-lumped model proposed in this paper and the P-Mesh code are used to calculate the S-parameters of a single-section coupler with four chamfered bends (on a 0.254 mm thick substrate with $\epsilon_r = 2.2$). The length of the coupled section is $\lambda/4$ at 10 GHz and the spacing between the parallel strips is 0.0127 mm. S_{21} results are plotted in Fig. 13 for frequencies ranging from 8 GHz to 12 GHz. S_{21} results using the planar-lumped model are plotted as curve 1. S_{21} results using the P-Mesh code are plotted as curve 2. S_{21} results using the P-Mesh code are obtained by taking three cells along the line width and five cells along the coupled line section. The total number of cells is 252. The cpu time needed to analyze this circuit at one frequency is 50 minutes on HP 375 workstation. However, the cpu time needed to analyze this circuit using the PLM is only around 1 minute. S_{21} results using quasistatic analysis (taking no discontinuity effects into account) are plotted as curve 3. The discrepancy in S_{21} results from the PLM and the P-Mesh code is only around 0.8 dB to 1 dB. P-Mesh code does not take the finite thickness of coupler strips into account and is therefore expected to yield a lower coupling. S_{21} results shown in Fig. 13 indicate that discontinuity effects on couplers cannot be neglected.

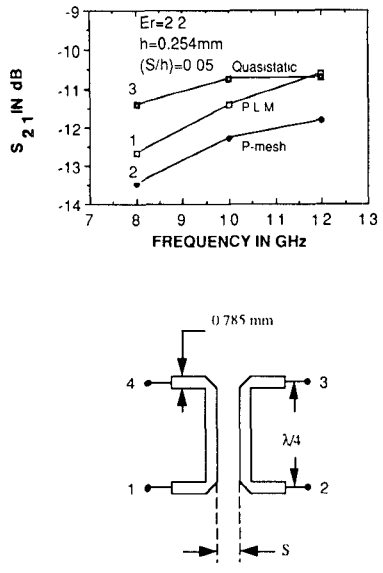

Fig. 13. Comparison of S_{21} results with fullwave analysis for a coupler with four chamfered bends.

VII. Discontinuity Effects in a Three-Section Coupler

A three-section 10 dB coupler was designed at 10 GHz on 0.101 mm gallium arsenide substrate ($\epsilon_r = 12.9$). The values of the even and odd mode capacitance (C_e) and (C_0), and even and odd mode effective dielectric constants ϵ_{re} and ϵ_{r0} were calculated using the Bryant and Weiss algorithm [7]. The coupler design was carried out using the procedure given in [13]. The configuration of the three-section coupler is shown in Fig. 14(a). The three-section coupler was broken down into regular elementary segments as shown in Fig. 14(b). The Z-matrices for segments 6 thru 9 are the same as for segments 1 through 4 and need not be computed separately.

The results calculated by the planar-lumped model are compared with conventional analysis (no discontinuity effects included) using transmission line analysis and with Touchstone software [14] taking discontinuity effects into account [15], [16]. The variation of the coupling factor S_{21} with frequency is shown in Fig. 15. S_{21} results using the planar-lumped model are shown as curve 1 of this figure. S_{21} results obtained using transmission line analysis are shown as curve 2. Touchstone [14] results taking discontinuity effects into account are shown as curve 3. The difference in S_{21} between the planar-lumped model (curve

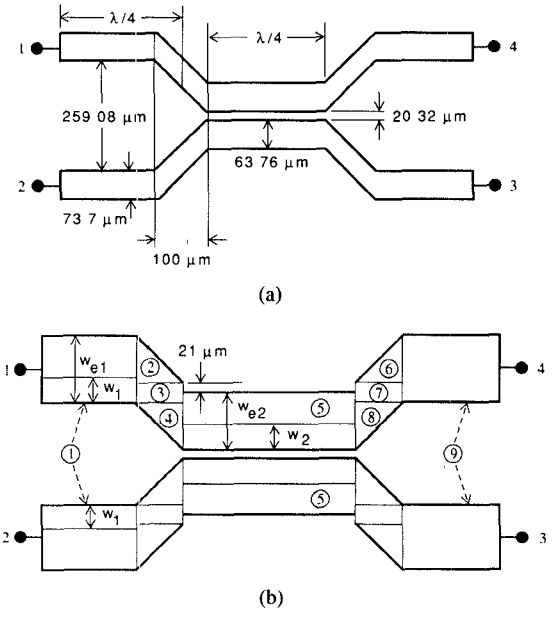

Fig. 14. Analysis of a 10 dB three-section coupler. (a) Layout. (b) Various segments of its model used for analysis.

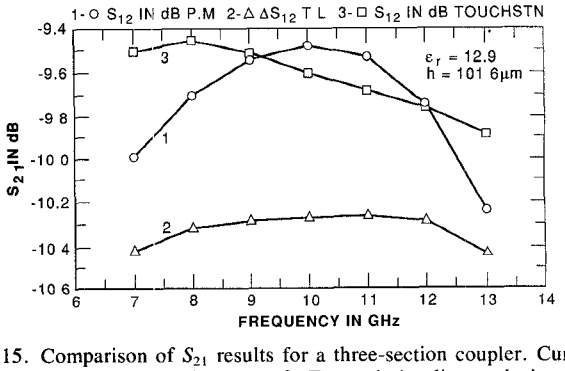

Fig. 15. Comparison of S_{21} results for a three-section coupler. Curve 1: Planar-lumped model results, curve 2: Transmission line analysis results. Curve 3: Touchstone results.

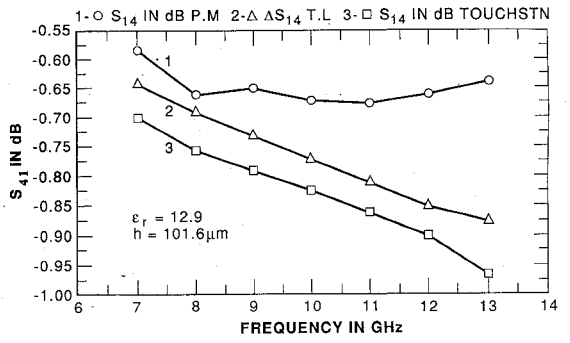

Fig. 16. Comparison of S_{41} results for a three-section coupler. Curve 1: P.L.M results. Curve 2: Transmission line analysis results. Curve 3: Touchstone results.

1), and transmission line analysis (curve 2) at 7 GHz is 0.4 dB and 0.75 dB at 10 GHz. The difference between results shown in curve 1 and curve 3 at 7 GHz is 0.03 dB and 1.1 dB at 13 GHz.

The differences in isolation values S_{31} between the planar-lumped model and transmission line analysis are 2 dB at 7 GHz and 20 dB at 13 GHz. The differences between S_{11} results obtained using the planar-lumped model and transmission line analysis are 1 dB at 7 GHz and 3 dB at 13 GHz. The differences between the planar-lumped model and the Touchstone results are 2 dB at 7 GHz and 3.2 dB at 13 GHz. Comparison of transmission S_{41} is shown in Fig. 16. The differences in S_{41} between the proposed model (curve 1) and transmission line analysis (curve 2) are 0.06 dB at 7 GHz and 0.27 dB at 13 GHz. The differences in S_{41} between curve 1 and Touchstone results (curve 3) are 0.12 dB at 7 GHz and 0.3 dB at 13 GHz. Modeling of losses plays a significant role in transmission coefficient S_{41}.

VIII. Conclusion

A novel modeling approach for characterization of coupled microstrip junction effects has been reported in this paper. This approach is an extension of the planar waveguide model used extensively for single microstrip line discontinuity reactance characterization. Good agreement with experimental results for chamfered bends (between coupled lines and single microstrip lines) is very encouraging. It has been verified that the planar-lumped model for coupled microstrips predicts accurately the higher-order modes also.

The proposed model has been applied to a number of different configurations. These include a single section coupler with chamfered bends at output ports and a three-section directional coupler. In all these cases, discontinuities are seen to cause appreciable change in performance. Comparison of sample results with fullwave analysis and with Touchstone results is included.

The proposed approach can be applied [17] for evaluating the radiation from coupled line discontinuities in the same manner as the planar waveguide model approach has been utilized [18] for study of radiation from single microstrip discontinuities.

Acknowledgment

The authors are grateful to Mr. Steve Yuan for making available the experimental results reported in Figs. 11 and 12 from the work carried out at Hughes Aircraft Company, Microwave Products Division, Torrance, CA.

References

[1] T. C. Edwards, *Foundation for Microstrip Circuit Design.* New York: Wiley, 1981, pp. 129–163.
[2] L. N. Dworsky, *Modern Transmission Line Theory and Applications.* Malabar, FL: Robert E. Krieger, 1988, pp. 109–136.
[3] R. H. Jansen, "High speed computation of single and coupled microstrip parameters including dispersion, high order modes, loss and finite strip thickness," *IEEE Trans. Microwave Theory Tech.*, vol. MTT-26, pp. 75–82, Feb. 1978.
[4] R. H. Jansen and N. H. L. Koster, "Accurate results on the end effect of single and coupled microstrip lines for use in microwave circuit design," *Arch. Elektr. Ubertr.*, vol. 34, pp. 453–459, 1980.
[5] G. Kompa and R. Mehran, "Planar waveguide model for computing microstrip components," *Electron. Lett.*, vol. 11, no. 9, pp. 459–460, 1975.
[6] R. Chadha and K. C. Gupta, "Compensation of discontinuities in planar transmission lines," *IEEE Trans. Microwave Theory Tech.*, vol. MTT-30, pp. 2151–2156, Dec. 1982.
[7] J. A. Weiss, "Microwave propagation on coupled pairs of microstrip transmission lines," in *Advances in Microwaves*, vol. 8, L. Young and H. Sobol, Eds. New York: Academic, 1974, pp. 295–320.
[8] C. Wei, Roger F. Harrington, Joseph R. Mauz, and Tapan Sarkar, "Multiconductor transmission lines in multilayered dielectric media," *IEEE Trans. Microwave Theory Tech.*, vol. MTT-32, pp. 439–450, Apr. 1984.
[9] K. C. Gupta, *Microwaves.* New York: Wiley Halstad Press, 1980, ch. 7.
[10] A. Benalla and K. C. Gupta, "Faster computation of Z matrices for rectangular segments in planar microwave circuits," *IEEE Trans. Microwave Theory Tech.*, vol. MTT-34, pp. 733–736, June 1986.
[11] H. J. Maramis and K. C. Gupta, "Planar model characterization of compensated microstrip bends," MIMICAD Tech. Report 1, University of Colorado at Boulder, 1989.
[12] J.-X. Zheng, "Electromagnetic modeling of microstrip circuit discontinuities and antennas of arbitrary shape," Ph.D. dissertation, University of Colorado, Dept. of Electrical and Computer Engineering, 1990.
[13] G. Matthaei, L. Young, and E. M. T. Jones, *Microwave Filters, Impedance-Matching Networks, and Coupling Structures.* Norwood, MA: Artech House, 1980, pp. 781–793.
[14] Touchstone Software, EEsof, Inc., Westlake Village, CA, Version 1.6, Oct. 1988.
[15] M. Kirshning, R. H. Jansen, and N. H. L. Koster, "Measurement and computer-aided modeling of microstrip discontinuities by an improved resonator method," in *IEEE MTT-S Int. Microwave Symp. Dig.*, May 1983, pp. 495–497.
[16] M. Kirschning and R. H. Jansen, "Accurate wide-range design equations for the frequency-dependent characteristic of parallel coupled lines," *IEEE Trans. Microwave Theory Tech.*, vol. MTT-32, pp. 83–90, Jan. 1984.
[17] A. Sabban, "Multiport network model for evaluating radiation loss and spurious coupling among microstrip discontinuities in microstrip circuits," Ph.D. dissertation, University of Colorado, Dept. of Electrical and Computer Engineering, 1991, Chapter 9.
[18] A. Sabban and K. C. Gupta, "Multiport network model for evaluating radiation loss and spurious coupling between discontinuities in microstrip circuits," in *1989 IEEE MTT-S Microwave Symp. Dig.*, vol. II, pp. 707–710.

Albert Sabban, photograph and biography not available at the time of publication.

K. C. Gupta (M'62–SM'74–F'88), photograph and biography not available at the time of publication.